Science World Journal Vol 14(No 2) 2019
www.scienceworldjournal.org
ISSN 1597-6343
Published by Faculty of Science, Kaduna State University

Full Length Research Article

COMPUTATIONS OF THE BAND STRUCTURE AND LINEAR OPTICAL PROPERTIES OF METHYLAMMONIUM BISMUTH BROMIDE AND METHYLAMMONIUM GALLUIM BROMIDE USING FHI-aims CODE

[1]S.G. Abdu*, [2]A. Shu'aibu, [3]M. Aboh and [4]M.S. Abubakar
[1,2,3,4]Department of Physics, Kaduna State University, Kaduna. PMB 2339, Kaduna, Nigeria
*Corresponding author email: sgabdul@kasu.edu.ng

ABSTRACT
Ab initio calculations for the Linear Macroscopic Dielectric analyses of $CH_3NH_3BiBr_3$ and $CH_3NH_3GaBr_3$ (having 8.33% dopant replacement percentage each) as possible replacements for the Lead based perovskite $CH_3NH_3PbBr_3$ were done in this work using Perdew–Burke–Ernzerhof functional of Density Functional Theory as implemented by FHI-aims Code. Optimized lattice constants were calculated for $CH_3NH_3BiBr_3$ and $CH_3NH_3GaBr_3$ to be 9.10 Å and 8.27 Å respectively. The Lowest Unoccupied Molecular Orbital (LUMO), Highest Occupied Molecular Orbital (HOMO) and calculated band gap, Band Structure and Density of States (DOS) plots were made to analyse the band structures of these crystals and they were found to be metallic with a band gap of 0.00018636 eV and 0.00022286 eV for $CH_3NH_3BiBr_3$ and $CH_3NH_3GaBr_3$ respectively. The imaginary and real parts of the inter-band and intra-band contribution to the linear dielectric tensor within the e imagi Random Phase Approximation (RPA) of the optical properties of these perovskites were calculated and an average dielectric tensor of 3.1209467 and 2.789173 was found for $CH_3NH_3BiBr_3$ and $CH_3NH_3GaBr_3$ respectively. From the absorption data and dielectric tensor components calculated, both materials have an average absorption peak at frequency of 16.5373nm at 1.006567 MeV, 16.2040nm at 1.227600 MeV respectively, across all cubic planes.

Keywords: Absorption Coefficient, Band Structure, DOS, $CH_3NH_3BiBr_3$, $CH_3NH_3GaBr_3$, DFT, Dielectric Tensor Components, FHI-aims.

INTRODUCTION

A lot of research in photovoltaic today focus on the applications of hybrid organic and inorganic methylammonium lead halide perovskite crystals $MAPbX_3$ (MA = CH_3NH_3; X = I, Br, Cl). The impressive optical properties of $MAPbI_3$ have been key to the success of hybrid perovskites as main component materials for photovoltaic cells. $MAPbI_3$ has a band gap located between 1.5 and 1.6 eV, practically close to the ideal given by Shockley-Queisser theory (the maximum single band gap efficiency is ~33.7% at 1.4 eV compared to $MAPbI_3$ at ~30% to 32%) (Aurélien *et al*, 2015). Associate this with its reported absorption coefficient of about 280 nm ($MAPbI_3$ absorbs approximately 80% of incident sun light under the band gap) makes it an admirable option for highly efficient thin film single junction photovoltaic cells (Aurélien *et al*, 2015). Further research into the optical properties is both practically and fundamentally important.

Still under debate are the theoretical optoelectronic properties of $MAPbX_3$ because calculated band structure plots and diagrams are not similar, and are dependent on the level of approximation used. Also from these basic gaps, the band distributions (band energy vs. crystal momentum) give different results based on different approximation levels.

Density Functional Theory usually underestimates the binding of occupied states, and also the splitting between occupied and unoccupied states. There is a noticeable misalignment of levels in certain heterogeneous materials because of errors in the quasiparticle level which depends on the element or compound in these heterogeneous materials. Corrections such as hybrid functionals, are purpose built to enhance the results of the band gap alone, but their exact contribution(s) to each band is vague. So, even though different computational methods yield similar band gaps, most of them give vague information about the electronic band structure of these perovskites.

Obtaining a band gap that shows considerable concord with experimental findings does not mean that the band dispersion is significant. Comparing all the major optical features in the visible range, and not only the band gap, is useful to assess the precision of any technique used to a new material and has not been yet reported for $MAPbX_3$ (Aurélien *et al,*2015).

More complexity comes from the fact that MA^+ is able to rotate, which is being thought to influence the photo-physical and electronic attributes of $MAPbX_3$. Molecular dynamics simulations (Frost *et al*, 2014) suggests that MA+ can have orientations along several different preferential orientations. MA+ reorientations between these alignments were shown to be compatible with Quasi-elastic neutron scattering measurements with activation energy of the order of 10 meV (Leguy *et al*, 2015). Good agreement between *ab initio* Quasiparticle Self-consistency GW (QSGW) simulations (G being Green's Function and W being the screened Coulomb interaction) and single crystal ellipsometry is shown in the spectral range that has all the optical transitions that are observable (1.2–5.5 eV) (Aurélien *et al*, 2015).

MATERIALS AND METHODS

DFT is one of the most popular and successful quantum mechanical approaches to matter. It is nowadays routinely applied for calculating- e.g. the binding energy of molecules in chemistry and the band structure of solids in physics. First applications relevant for fields traditionally considered more distant from quantum mechanics, such as biology and mineralogy are beginning to appear. Superconductivity, atoms in the focus of strong laser pulses, relativistic effects in heavy elements and in atomic nuclei, classical liquids, and magnetic properties of alloys have all been studied with DFT.

DFT owes this versatility to the generality of its fundamental

concepts and the flexibility one has in implementing them. In spite of this flexibility and generality, DFT is based on quite a rigid conceptual framework. This section introduces some aspects of this framework in general terms.

To get a first idea of what density-functional theory is about, it is useful to take a step back and recall some elementary quantum mechanics. In quantum mechanics we learn that all information we can possibly have about a given system is contained in the system's wave function, Ψ. Here we will exclusively be concerned with the electronic structure of atoms, molecules and solids. The nuclear degrees of freedom (e.g., the crystal lattice in a solid) appear only in the form of a potential v(r) acting on the electrons, so that the wave function depends only on the electronic coordinates. Nonrelativistically, this wave function is calculated from Schrödinger's equation, which for a single electron moving in a potential v(r) reads

$$\left[-\frac{\hbar^2\nabla^2}{2m}+v(r)\right]\Psi(r)=\epsilon\Psi(r) \qquad (1)$$

If there is more than one electron (i.e., one has a many-body problem), Schrödinger's equation then becomes:

$$\left[\sum_i^N\left(-\frac{\hbar^2\nabla_I^2}{2m}+v(r_I)\right)+\sum_{i<j}U(r_i,r_j)\right]\Psi(r_1,r_2\ldots,r_N)=\epsilon\Psi(r_1,r_2\ldots,r_N) \qquad (2)$$

where N is the number of electrons and $U(r_i, r_j)$ is the electron-electron interaction. For a Coulomb system (the only type of system we consider here) one has

$$\hat{U}=\sum_{i<j}U(r_i,r_j)=\sum_{i<j}\frac{q^2}{|r_i-r_j|} \qquad (3)$$

Note that this is the same operator for any system of particles interacting via the Coulomb interaction, just as the kinetic energy operator

$$\hat{T}=-\frac{\hbar^2}{2m}\sum_i\nabla_i^2 \qquad (4)$$

is the same for any nonrelativistic system. One sometimes says that $\hat{T}$ and $\hat{U}$ are 'universal', while $\hat{V}$ is system-dependent, or 'non-universal'. Whether our system is an atom, a molecule, or a solid thus depends only on the potential $v(r_i)$. For an atom, e.g:

$$\hat{V}=\sum_i v(r_i)=\sum_i\frac{Qq}{|r_i-\boldsymbol{R}|} \qquad (5)$$

where "Q" is the nuclear charge and "**R**" the nuclear position. When dealing with a single atom, **R** is usually taken to be the zero of the coordinate system. For a molecule or a solid one has

$$\hat{V}=\sum_i v(r_i)=\sum_{ik}\frac{Q_kq}{|r_i-\boldsymbol{R}_k|} \qquad (6)$$

where the sum on k extends over all nuclei in the system, each with charge $Q_k = Z_k e$ and position $\mathbf{R}_k$. It is only the spatial arrangement of the $\mathbf{R}_k$ (together with the corresponding boundary conditions) that distinguishes, fundamentally, a molecule from a solid. Similarly, it is only through the term $\hat{U}$ that the (essentially simple) single-body quantum mechanics of Eq. (1) differs from the extremely complex many-body problem posed by Eq. (2). These properties are built into DFT in a very fundamental way.

It is easy enough to calculate the total energy of a single particle whose wave function is known. An isolated particle poses an ideal case for the application of Schrödinger's equation. What if a realistic case is considered? A simple calculation becomes really cumbersome and almost impossible to do in a lifetime, by the greatest scientific minds. For example, consider 1 gram of Sodium. Sodium has atomic number 11 and mass number 22.990. 1 gram of sodium contains approximately 6.025×10^{23} sodium molecules. Sodium has 22 nucleons and 11 electrons thus it has 33 particles constituting its atom. Assuming that neutrons do not interact with electrons and protons, we have 11 protons and 11 electrons interacting with each other for an atom of sodium. Realistically, 1 gram of Sodium contains approximately 66.275×10^{23} protons and 66.275×10^{23} electrons. That is, 1 gram of Sodium contains approximately 13,255,000,000,000,000,000,000,000 particles interacting with each other. Calculating the total energy contained in 1 gram of sodium requires resolving the Schrödinger equation for each particle interaction (electron-electron, proton-electron) for 13 billion, trillion particles having individual wave-functions varying from particle to particle. It obviously can be done. But not by one person, and definitely not in one lifetime. Even super-computers would take years to accomplish this feat. This is just one relatively simple realistic case. Consider 1Kg of TiO_2 for example. The problem becomes really troubling to consider. This is where DFT comes in. Simply approximating this many-body problem.

"This is a remarkable theory that allows one to replace the complicated N-electron wave function Ψ (x_1, x_2, ..., x_N) and the associated Schrödinger equation by the much simpler electron density ρ(r) and its associated calculational scheme. Remarkable indeed!" (Parr and Yang, 1989).

This research was done using a compiled binary of the "scalapack.mpi" version of Fritz Haber Institute *ab initio* molecular simulation (FHI-aims) code (FHI-aims 171221_1) on the ELSI Electronic Structure Infrastructure (Yu *et al*, 2018) and ELPA library (Marek *et al*, 2014) to calculate the energies for the structural optimization of $MABiBr_3$ and $MAGaBr_3$ molecules, using additional software like Grace (Graphing Advanced Computation and Exploration of data) to graphically represent data. Regarding computer specifications, the computer used for this calculation was a Dell Inspiron N5110 notebook PC that had a quad-core Intel(R) Core(TM) i5-2430M CPU clocking up to 2.79GHz, with 8 GB of RAM running on the Linux-based Ubuntu 16.04 LTS.

RESULTS AND DISCUSSION

The results obtained from the geometry relaxation and the lattice constant optimization were used as the fundamental conditioning criteria for the Band Structure and Density of States (DOS) calculations for $CH_3NH_3BiBr_3$ and $CH_3NH_3GaBr_3$ using FHI-aims code. Since perovskites are naturally cubic ($CH_3NH_3PbBr_3$ is cubic in nature), $CH_3NH_3BiBr_3$ and $CH_3NH_3GaBr_3$ should also be cubic assuming they are perovskites. A simple check to see if they are naturally Body-Centered Cubic (BCC) or Face-Centered Cubic (FCC) structures was done by running energy calculations of the two aforementioned structures. The structure with the lower calculated total energy in eV is the more stable structure and should be the natural state of the compounds.

Afterwards, band structure calculations were implemented using fairly high convergent criteria; 12x12x12 K-grid and 9x9x9 DOS K-

grid and the default suggestions for Light Atomic Species (using high convergence criteria, "Tight" or "Really Tight" for atomic species was not done because it was too computationally expensive for the computer hardware components used). The corresponding band structure was calculated for symmetry k-points L, Γ, X, W and K which correspond to the points required for band structure plots for cubic systems.

The Lowest Unoccupied Molecular Orbital (LUMO), Highest Occupied Molecular Orbital (HOMO) and calculated band gap is tabulated below. Band Structure and DOS plots were done to analyse the band structures of these crystals to see if they are Insulators (insulators have really high band gap in eV the Fermi level), Semiconductors (semiconductors have a relatively small band gap at the Fermi level as compared with insulators), or Metallic (have little or no band gap at the Fermi level). The Band structure and DOS plots resulting from the band structure calculations are as shown in Figure 3 (a) and Figure 3 (b).

The resulting plots show that there are bands at the Fermi level for both $CH_3NH_3BiBr_3$ and $CH_3NH_3GaBr_3$ thus there is a very small band gap suggesting that these materials are both metallic and are not fit for use as photoconductive materials in the fabrication of DSSCs. Bismuth and Gallium may be good substitutes for Lead in other materials but this study shows that they are not good replacements for Lead in the $MAPbBr_3$ perovskite crystal structure. The table below shows the calculated LUMO, HOMO, and Band gap in eV, and the suggested material type based on the band gaps.

TABLE 1: Calculated LUMO, HOMO and Band Gap Energies

MATERIAL	LUMO (eV)	HOMO (eV)	Band gap (eV)	Material Type
$CH_3NH_3BiBr_3$	-4.98522978	-4.98541615	0.00018636	Metallic
$CH_3NH_3GaBr_3$	-5.07541462	-5.07563748	0.00022286	Metallic

Figure 3 shows that $MABiBr_3$ and $MAGaBr_3$ are metallic in nature considering the Gaussian broadening method and the convergent criteria used (PBE_vdw). Although the previous section shows that these materials are not suitable for photovoltaic use based on their band structure, this section is a report of the calculated optical properties regardless. After the calculations implemented by setting the basic parameters for calculating the imaginary and real part of the inter-band and intra-band contribution to the linear dielectric tensor within the RPA approximation of the optical properties of these crystals were done, the graphs of real and imaginary components of the linear macroscopic dielectric tensor ($Re(\varepsilon_r)$ and $Im(\varepsilon_{Im})$ respectively) against plasma frequency (ω) in eV for cubic directions [100], [010], and [001] were plotted and are shown in figure 4(a) and 4(b). The dielectric constant (relative permittivity) which is value of the real part of the linear dielectric tensor at frequency equals to zero (i.e.$R[\epsilon_r(\omega=0)]$ for each of the above direction should be given. But in order to avoid numerical integration errors caused by including 0 eV energy, the minimum energy (ω_{min}) are automatically set to a specific value corresponding to the broadening width used (broadening width/10.0) (Blum *et al*, 2016). Thus for Gaussian broadening function used in this calculation, broadening width is 0.05eV, meaning that dielectric constant will be calculated at $R[\epsilon_r(\omega=0.005)]$. Below are the graphs resulting from the dielectric calculations.

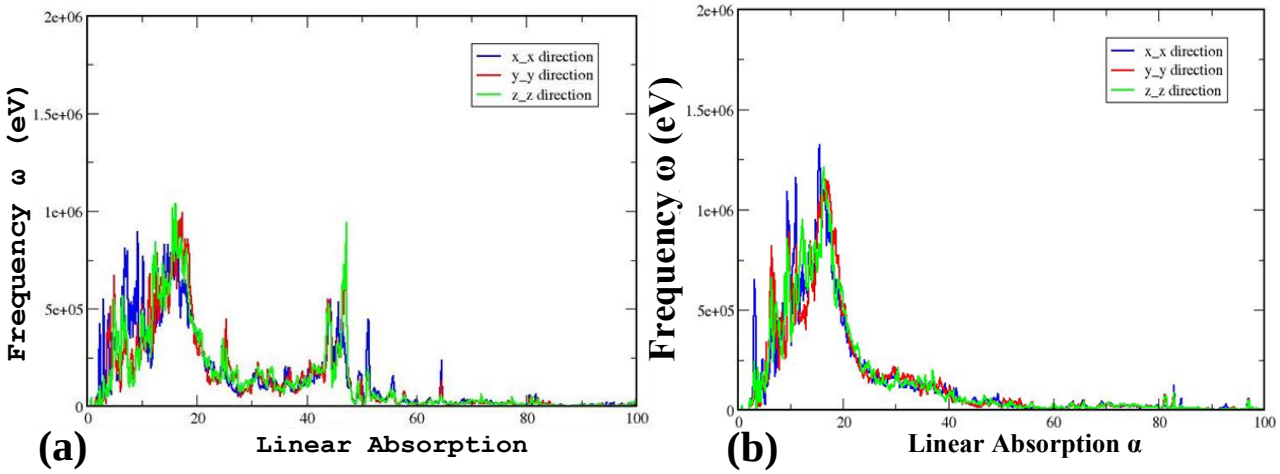

Figure 4 a): Linear absorption (α) plot with respect to Plasma Frequency (ω) for $CH_3NH_3BiBr_3$.Using Gaussian broadening method showing x_x direction [100], y_y direction [010], and z_z direction [001].

b): Linear absorption (α) plot with respect to Plasma Frequency (ω) for $CH_3NH_3GaBr_3$.Using Gaussian broadening method showing x_x direction [100], y_y direction [010], and z_z direction [001].

Science World Journal Vol 14(No 2) 2019
www.scienceworldjournal.org
ISSN 1597-6343
Published by Faculty of Science, Kaduna State University

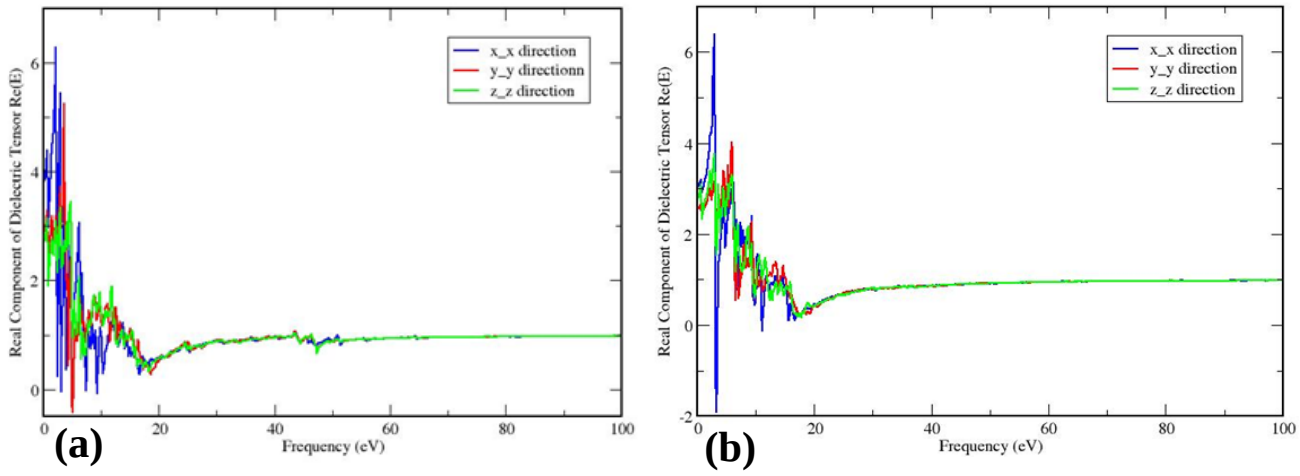

Figure 5 a): Real Component of Linear macroscopic dielectric tensor (ε) vs plasma frequency (ω) for $CH_3NH_3BiBr_3$.Using Gaussian broadening method showing x_x direction [100], y_y direction [010], and z_z direction [001].

b): Real Component of Linear macroscopic dielectric tensor (ε) vs plasma frequency (ω) for $CH_3NH_3GaBr_3$. Using Gaussian broadening method showing x_x direction [100], y_y direction [010], and z_z direction [001].

The calculated values for the dielectric constants are represented in the table 2 below:

Table 2: Calculated Dielectric Tensor Constants

Material	$Re[\varepsilon_r(\omega=0.005)]$ Gaussian		
	x_x direction [100]	y_y direction [010]	z_z direction [001]
$CH_3NH_3BiBr_3$	3.79185	2.87548	2.69551
$CH_3NH_3GaBr_3$	3.03730	2.54869	2.78153

Table 3: *Calculated Absorption Peaks*

Material	x_x direction [100]		y_y direction [010]		z_z direction [001]	
	ω(MeV)	α(nm)	ω(MeV)	α(nm)	ω(MeV)	α(nm)
$CH_3NH_3BiBr_3$	0.991640	16.2040	0.992560	17.3040	1.035500	16.1040
$CH_3NH_3GaBr_3$	1.322200	15.6040	1.151700	16.7040	1.208900	16.3040

Table 3 above shows the linear absorption peaks for $CH_3NH_3BiBr_3$ and $CH_3NH_3GaBr_3$ both giving and average absorption peak at peak frequency of 16.5373nm at 1.006567 MeV, and 16.2040nm at 1.227600 MeV respectively, across all cubic planes. From Figure, it can be observed that $CH_3NH_3BiBr_3$ gives an absorption range from about 4nm to 48nm and $CH_3NH_3GaBr_3$ gives a range from 5nm to 42nm, and Figure 5 shows an average calculated dielectric tensor of 3.1209467 and 2.789173, respectively.

REFERENCES

Abdulsalam H. and Babaji G. (2018), "First Principle Study on Lead-free $CH_3NH_3GeI_3$ and $CH_3NH_3GeBr_3$ Perovskites Using FHI-aims Code". *Cornell University Library*, https://arxiv.org/abs/1806.10945, 2018.

Andreas G., Martijn M., Judith H., Laurids S. and Georg K. (2009), "Making the random phase approximation to electronic correlation accurate". *J. Chem. Phys.*, 131:154115, 2009.

Auckenthaler T., Blum, V., Bungartz, H.-J., Huckle, T., Johanni, R., Kraemer, L., Lang, B., Lederer, H., and Willems, P. R., (2011), "Parallel solution of partial symmetric eigenvalue problems from electronic structure calculations". Parallel Computing 37, 783-794. http://dx.doi.org/10.1016/j.parco.2011.05.002, 2011.

Blum, V., Gehrke, R., Hanke, F., Havu, P., Havu, V., Ren, X., Reuter, K., and Scheffler, M., (2009), "Ab initio molecular simulations with numeric atom-centred orbitals (FHI-aims Manual)", *Computer Physics Communications*, 180:2175-2196, 2009.

Blum V., Gehrke R., Hanke F., Havu P., Havu V., Ren X., Reuter K., and Scheffler M., (2016), Ab initio molecular simulations with numeric atom-centered orbitals (FHI-aims Manual), *Comp. Phys. Comm.*, 180:2175, 2016.

Dresselhaus, M. S., (1997), "Solid State Physics Part II - Optical Properties of Solids".

Frost, J. M., Butler, K. T., and Walsh, A., (2014), *APL Mater*, 2, 081506–081516, 2014.

Kai-Hung, W., Liang-Chen, L., Muthaiah, S. & Kien, W. S. (2017), "Structural and Photophysical Properties of Methylammonium Lead Tribromide ($MAPbBr_3$) Single Crystals", *Scientific Reports*, www.nature.com/scientificreports/, date accessed 21/05/2018.

Leguy, A. M. A., Frost,J. M., McMahon, A. P., Sakai, V. G., Kochelmann, W., Law, C., Li, X., Foglia, F., Walsh, A., O'Regan, B. C., Nelson, J., Cabral, J. T. and Barnes, P. R. F., *Nat. Commun.,* 2015, 6, 7124.

Marek, A., Blum, V., Johanni, R., Havu, V., Lang, B., Auckenthaler, T., Heinecke, A., Bungartz, H-J., and Lederer, H., (2014), "The ELPA Library - Scalable Parallel Eigenvalue Solutions for Electronic Structure Theory and Computational Science". *The Journal of Physics: Condensed Matter 26*, 213201, 2014. http://dx.doi.org/10.1088/0953-8984/26/21/213201

M¨oller, S. and Weiser, G. (1999). Photoconductivity of polydiacetylene chains in polymer and monomer single crystals. *Chem. Phys.*, **246**, 483-94.

Parr, R. G. and Yang, W. (1989), "Density-Functional Theory of Atoms and Molecules", Oxford University Press, Inc., New York. 47-53 1989.

Ren, X., Rinke, P., Blum, V., Wieferink, J., Tkatchenko, A., Sanfilippo, A., Reuter, K., and Scheffler, M., (2012). *New Journal of Physics 14*, 053020.

Ren, X., Tkatchenko A., Rinke, P., and Scheffler, M., (2011), "Beyond the random-phase approximation for the electron correlation energy: The importance of single excitations". *Phys. Rev. Lett.*, 106:153003, 2011.

Yu, P.Y., Cardona, M., (2010), "Fundamentals of Semiconductors" 4th ed., DOI 10.1007/978-3-642-00710-1_2, © Springer-Verlag Berlin Heidelberg 2010 19-103

Yu, V. W-z., Corsetti, F., Garcia, A., Huhn, W. P., Jacquelin, M., Jia, W., Lange, B., Lin, L., Lu, J., Mi, W., Seifitokaldani, A., Vazquez-Mayagoitia, A., Yang, C., Yang, H., and Blum, V., (2018), "ELSI: A unified software interface for Kohn-Sham electronic structure solvers". *Computer Physics Communications 222*, 267-285. http://dx.doi.org/10.1016/j.cpc.2017.09.007, 2018.